Supplemental Information

Supplemental Figures S1-S7

Supplemental Table

A

gRNA target 1: 5'...GGGAAAGAGACCCATTTAAACGGTGGCGGGAACATCATTTT...3'

sgRNA target 2: 5'...GGTGCGGACCAAAGCAAACTACGTTCCAGGAGCCT...3'

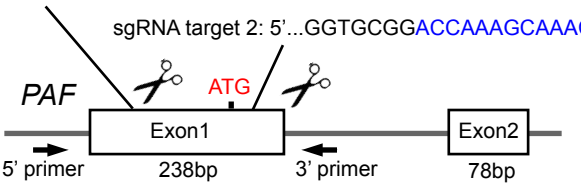

B

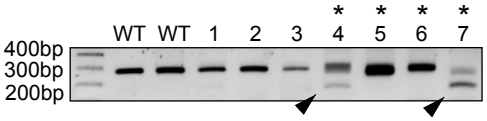

C

….AGCGCGCGGGAAAGAGACCCATTTAAACGGT- - - - - - - ACTACGTTCCAGGAGCCTACA….

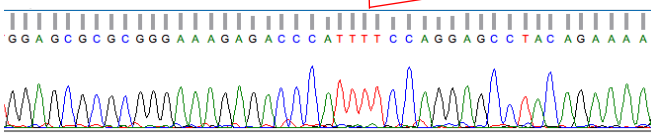

strain 4: null allele
118 bp deletion

….GAGCGCGCGGGAAAGAGACCCATTTAAA- - - - - - -TACGTTCCAGGAGCCTACAGAAAAG…

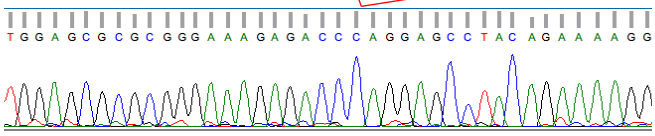

strain 7 : null allele
125 bp deletion

D

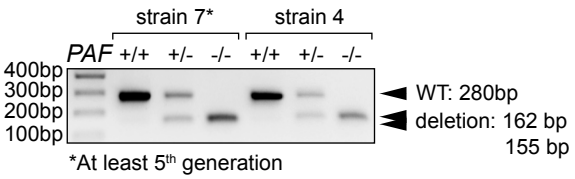

*At least 5th generation

E

Sequencing results of potential off-target regions

Sequence	Mismatches	Gene	Locus	Mutation (-30~+30)	
GTTCCCGGCACTTTTTAATTAAG	4MMs [8:12:13:19]	NM_001099298	chr2:+65604588	No	gRNA 1 potential off-target
GCTCCCGCCACCGCTTGAACAAG	4MMs [2:14:17:20]	NM_026577	chr16:+62846516	No	
GCCAGAGCAAAATATGTTCCAAG	4MMs [1:5:12:15]	NM_146283	chr13:-21628884	No	gRNA 2 potential off-target
ACCAAATCCCACCACGTTCCAGG	4MMs [7:9:10:13]	NM_175177	chr16:+31458336	No	
ACCTAAGCATCCTACCTTCCAAG	4MMs [4:10:11:16]	NM_001177565	chr12:+88858284	No	
ACCTAAGCATGCTACCTTCCAAG	4MMs [4:10:11:16]	NM_010120	chr18:+46767791	No	
ACGAAAGGAAACTACGGGCCTAG	4MMs [3:8:17:18]	NM_019750	chr9:+107482963	No	
ACCAAATCACACTATGTTCTTGG	4MMs [7:10:15:20]	NM_172925	chr9:+77504809	No	
ACCATAGCAAAATATGCTCCCAG	4MMs [5:12:15:17]	NM_001029934	chr11:-84839164	No	
ACAAAAGCAAACCACCTTACCAG	4MMs [3:13:16:19]	NM_011916	chr9:-95948855	No	
GCCAAAGCAAACTTCTTTCGCGG	4MMs [1:14:16:20]	NM_016974	chr7:-52960515	No	
ACCAAAGCACAGTTCTTTCCAGG	4MMs [10:12:14:16]	NM_177863	chr4:+82546380	No	
AGCAAAGCAAACTGTATTCCCAG	4MMs [2:14:15:16]	NM_001048192	chr5:+31193044	No	
ACCAAAGCAAACTACTGAGCAAG	4MMs [16:17:18:19	NM_001166065	chr13:+97705	No	

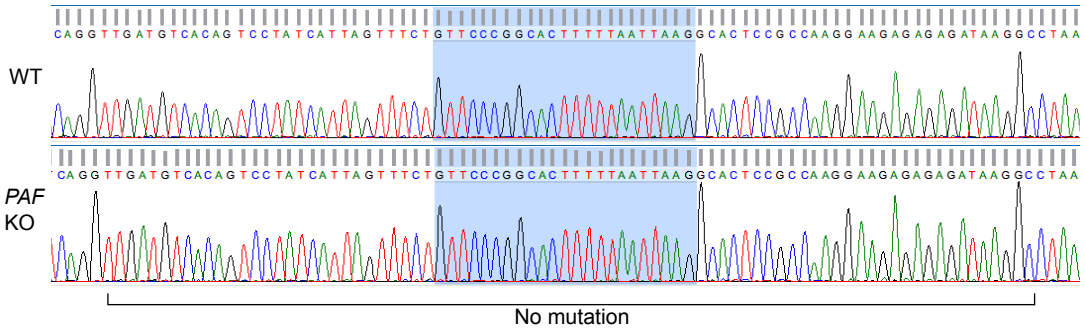

gRNA 1 potential off-target:
GTTCCCGGCACTTTTTAATTAAG

Figure S1. Establishment of *PAF* KO Mice (related to Figure 2)

(A) Schematic view of targeting Exon 1 of *PAF* gene by two guide RNAs. Arrows indicate the 5'- and 3'- primer pairs for genotyping.

(B) Detection of *PAF* deleted chromosome by PCR genotyping. Four pups showed band shift among the seven pups from zygotes injection. Asterisks indicate pups harboring deleted alleles. Strain 4 and 7 showed the small size PCR bands (large size of deletion).

(C) Sequencing analysis of strain 4 and 7. Strain 4 and 7 carried 118bp and 125bp deletion between the two gRNAs targeted regions, respectively. Because deleted region contained first ATG sequences, chromosomes harboring deletion in strain 4 and 7 are null.

(D) Generation of *PAF* KO founder from strain 4 and 7. At least 5 successive breeding with C57BL/6 were conducted for experiments.

(E) Sequencing result of off-target regions. Predicted off-targets of gRNAs (MIT CRISPR Designer) were sequenced using the founder strains. No mutation was detected in +30~-30 region of off-targets. One example of potential off-target sequencing was shown (the lower panel).

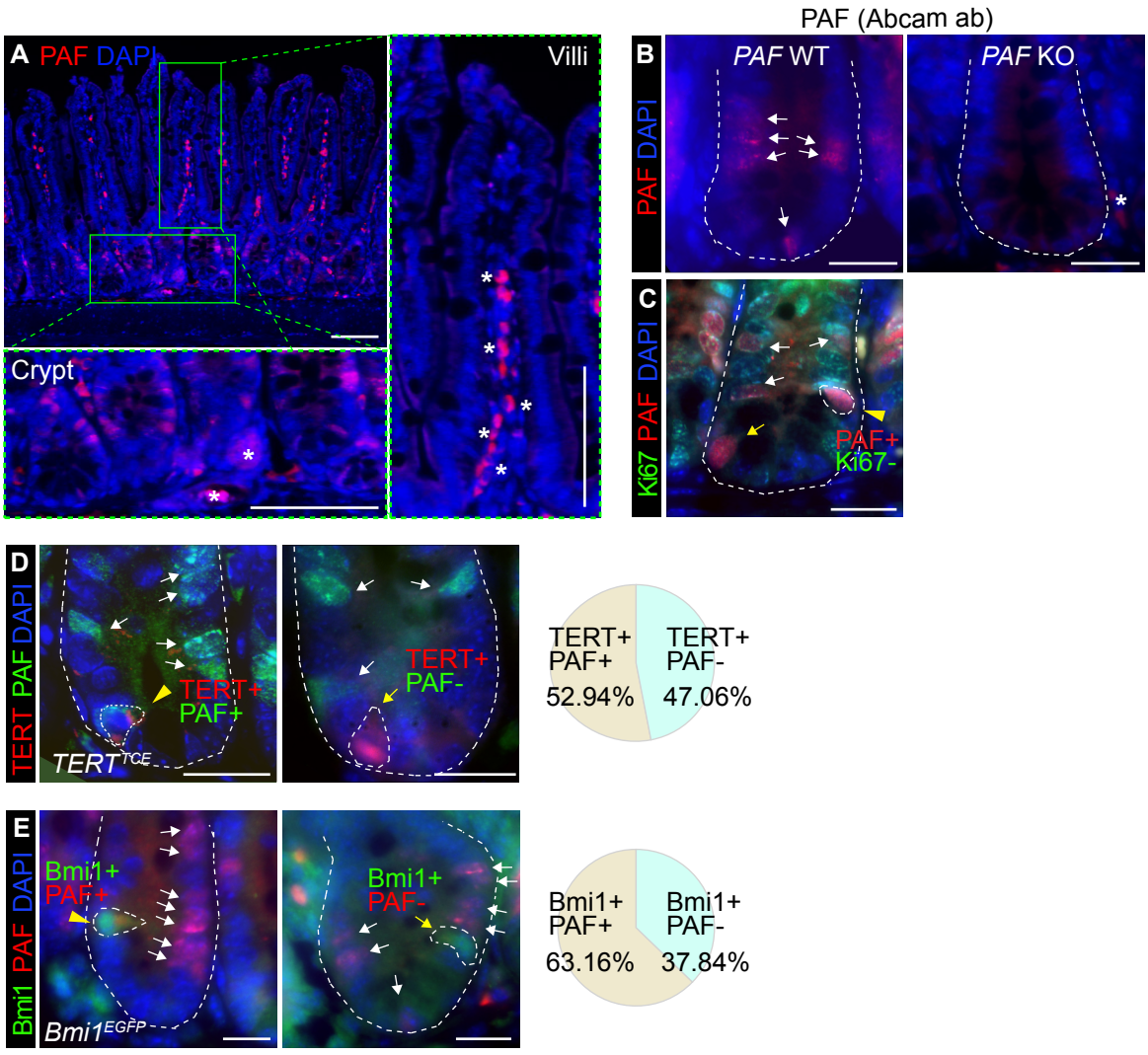
PAF (Abcam ab)
A PAF DAPI
Villi
Crypt
B
PAF DAPI
PAF WT
PAF KO
C
Ki67 PAF DAPI
PAF+
Ki67-
D
TERT PAF DAPI
TERT+
PAF+
TERT^TCE
TERT+
PAF-
TERT+
PAF+
52.94%
TERT+
PAF-
47.06%
E
Bmi1 PAF DAPI
Bmi1+
PAF+
Bmi1^EGFP
Bmi1+
PAF-
Bmi1+
PAF+
63.16%
Bmi1+
PAF-
37.84%

Figure S2. Expression of PAF in Intestinal Crypts (related to Figure 2)

(A) PAF+ cell in the mouse small intestine. Mice were analyzed for immunofluorescent (IF) of PAF (red) staining. Green boxes indicate the magnification view of Villi and Crypt. Asterisks mark non-specific staining signals. Scale bars=100μm.

(B) Validation of PAF expression by the alternative anti-PAF antibody. Anti-PAF [ab56773] antibody showed the same pattern of PAF expression in *PAF* WT and KO mice as shown in Figure 2A using Anti-PAF [G-11].

(C) PAF+:Ki67- cells in the crypt. Co-immunostaining of mouse small intestine (*PAF* WT) for PAF and Ki67. White arrows: PAF+:Ki67+ cells; yellow arrows: PAF+:Ki67+ CBC cells; arrowhead: PAF+:Ki67- cell.

(D, E) PAF expression in TERT+ and Bmi1+ cells. Co-immunostaining of *TERT-Tdtomato-CreERT2* knockin mouse for PAF and tdTomato (D); or *Bmi1-EGFP* knockin mouse intestine samples for PAF and Bmi1 (E); Arrowheads: PAF+:TERT+ (D) and PAF+:Bmi1+ (E) cells; Arrows: PAF-:TERT+ (D) and PAF-:Bmi1+ (E) cells; The numbers indicate % of PAF+:TERT+ (D) and PAF+:Bmi1+ (E) cell from the total numbers (TERT+ or Bmi1+ cells). Asterisks mark non-specific staining signals. Scale bars=20μm.

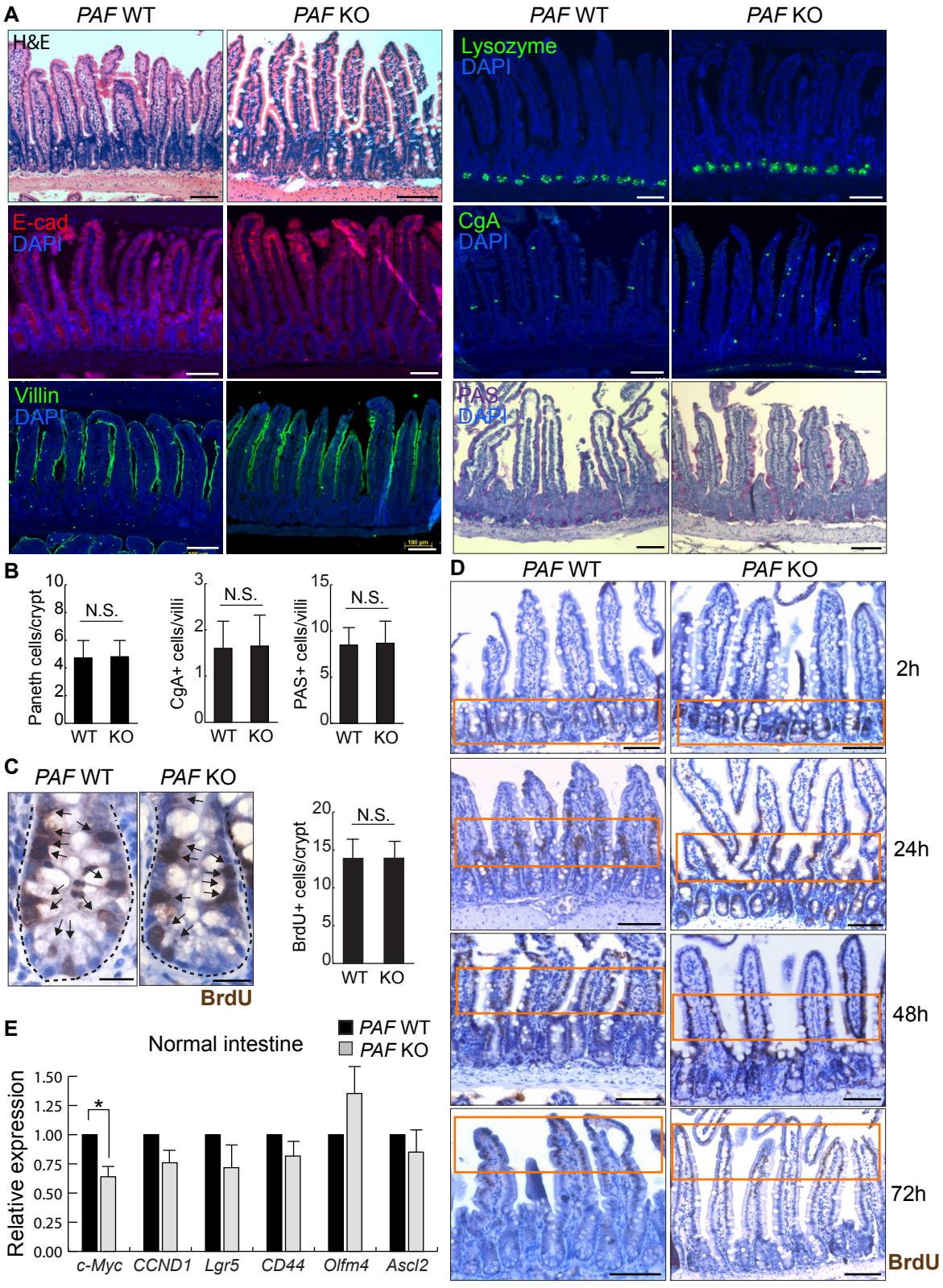
A
PAF WT
PAF KO
PAF WT
PAF KO
H&E
Lysozyme
DAPI
E-cad
DAPI
CgA
DAPI
Villin
DAPI
PAS
DAPI
B
Paneth cells/crypt
N.S.
WT KO
CgA+ cells/villi
N.S.
WT KO
PAS+ cells/villi
N.S.
WT KO
C
PAF WT
PAF KO
BrdU
BrdU+ cells/crypt
N.S.
WT KO
D
PAF WT
PAF KO
2h
24h
48h
72h
BrdU
E
Normal intestine
PAF WT
PAF KO
Relative expression
c-Myc
CCND1
Lgr5
CD44
Olfm4
Ascl2

Figure S3. Analysis of *PAF* KO Intestine (related to Figure 3)

(A) Comparison of WT and *PAF* KO intestine in the normal condition. H&E staining and immunostaining for E-cad (epithelial cell marker), Villin (intestinal epithelial marker), Lysozyme (the Paneth cell marker), CgA (Neuroendocrine cell marker), and PAS (Goblet cell marker) in WT and *PAF* KO intestines. Scale bars=100μm.

(B) Analysis of Lysozyme+ (the Paneth cell) in the crypt. Quantification of CgA+ (Neuroendocrine cell), and PAS+ (Goblet cell marker) in the intestine. At least 40 fields were counted.

(C) Quantification of proliferation cell in WT and *PAF* KO intestinal crypts. BrdU staining after 2h BrdU induction. The right graph: Quantification of BrdU+ cell in the crypts of *PAF* WT and KO mice. Scale bar=20μm.

(D) Tracing the migration of BrdU+ cells in the crypts. BrdU migration assays of *PAF* WT and KO mice. Green boxes indicate the migrating BrdU+ cells. Scale bars=100μm.

(E) Comparison of gene expression levels relating intestinal homeostasis in *PAF* WT and KO mice. qRT-PCR was conducted using crypt fraction from *PAF* WT and KO mice. Of note, the slight decrease in c-*Myc* expression was detected. Asterisks: $P<0.05$.

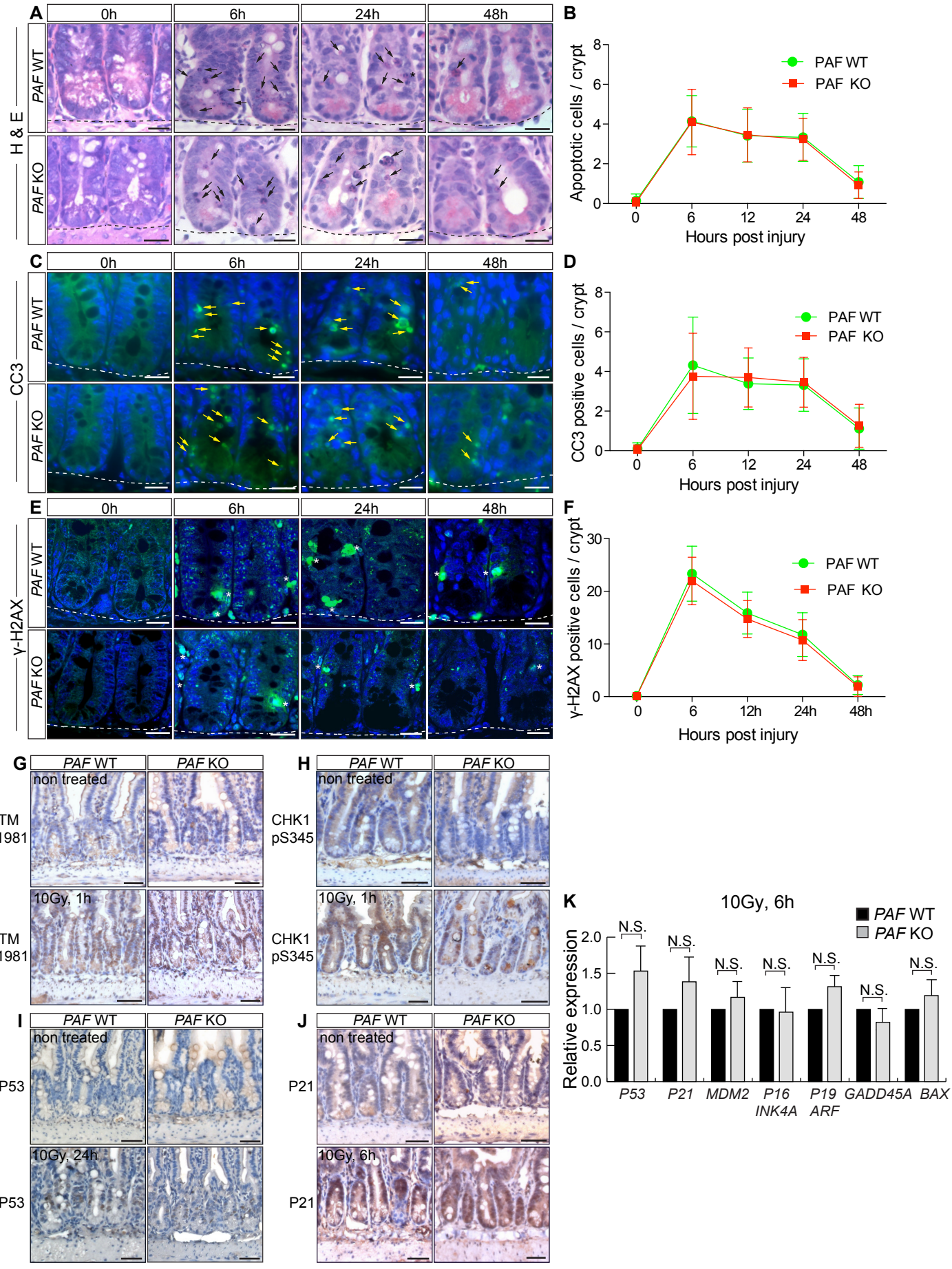
A
0h
6h
24h
48h
H & E
PAF WT
PAF KO
B
Apoptotic cells / crypt
PAF WT
PAF KO
Hours post injury
C
CC3
D
CC3 positive cells / crypt
E
γ-H2AX
F
γ-H2AX positive cells / crypt
G
PAF WT
PAF KO
non treated
ATM pS1981
10Gy, 1h
H
CHK1 pS345
I
P53
10Gy, 24h
J
P21
10Gy, 6h
K
10Gy, 6h
Relative expression
N.S.
P53
P21
MDM2
P16 INK4A
P19 ARF
GADD45A
BAX

Figure S4. *PAF* KO Does Not Affect Intestinal Cell Death and DNA Damage Responses (related to Figure 3)

(A-D) No differences in cell death after IR injury between *PAF* WT and KO mice. Apoptotic bodies in the crypts were analyzed at the indicated time points (0h, 6h, 24h, 48h) (A); Quantification of apoptotic bodies in the crypt (B); IF staining of *PAF* WT and KO mice were performed for cleaved-Caspase 3 (CC3), a marker for apoptosis (C) at the indicated time points (0h, 6h, 24h, 48h); Quantification of CC3 in the crypt (D). Scale bars=20μm. The representative images were shown from at least three mice.

(E, F) No differences in DNA damage (γ-H2AX) response after IR injury between *PAF* WT and KO mice. DNA double-strand break was analyzed by IF staining using γ-H2AX between the *PAF* WT and KO mice crypts at the indicated time points (0h, 6h, 24h, 48h) (E); Quantification of γ-H2AX in the crypt from *PAF* WT and KO mice (F). Scale bars=20μm. The representative images were shown from at least three mice.

(G, H) The early time DNA damage response was not changed in *PAF* KO crypt. IHC for ATM pS1981 in the *PAF* WT and KO mice crypts after irradiation injury (1h, 10Gy)(G); IHC for CHK1 pS345, a downstream target of ATR/ATM DNA damage response, in the *PAF* WT and KO mice crypts after irradiation injury (1h, 10Gy)(H). Scale bars=50μm.

(I, J) Myc-related DNA damage response pathways were not changed in *PAF* KO crypt. IHC for P53 (I) (24h, 10Gy) and P21 (J) (6h, 10Gy) in the *PAF* WT and KO mice crypts after irradiation injury. Scale bars=50μm.

(K) Gene expression analysis of Myc-related DNA damage response. *PAF* WT and *PAF* KO crypts (6h, 10Gy) were analyzed for qRT-PCR. At least three experiments were conducted. qRT-PCR was conducted using indicating primers.

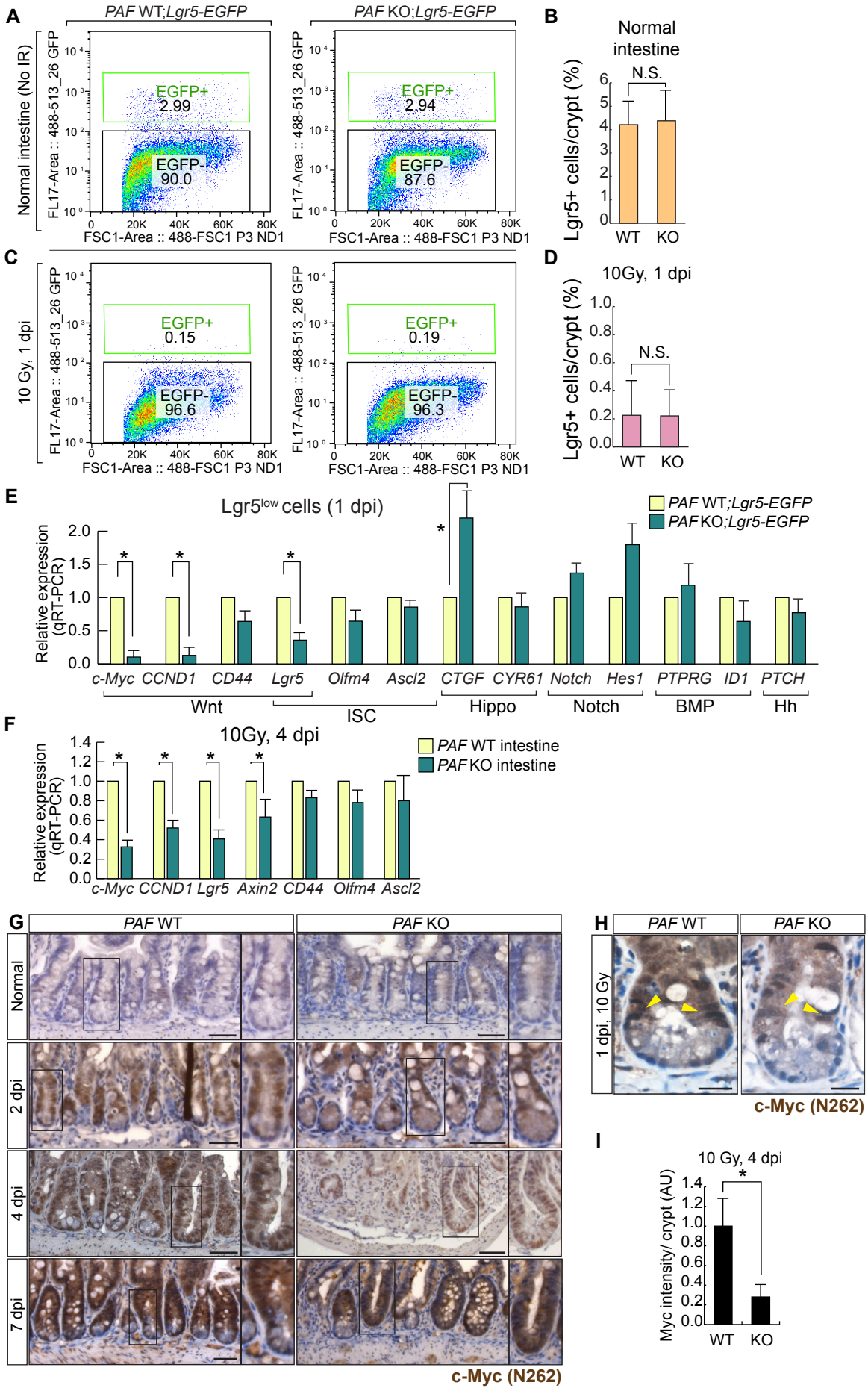
A
PAF WT;Lgr5-EGFP
PAF KO;Lgr5-EGFP
Normal intestine (No IR)
FL17-Area :: 488-513_26 GFP
FSC1-Area :: 488-FSC1 P3 ND1
EGFP+ 2.99
EGFP- 90.0
EGFP+ 2.94
EGFP- 87.6
B
Normal intestine
N.S.
Lgr5+ cells/crypt (%)
WT
KO
C
10 Gy, 1 dpi
EGFP+ 0.15
EGFP- 96.6
EGFP+ 0.19
EGFP- 96.3
D
10Gy, 1 dpi
N.S.
Lgr5+ cells/crypt (%)
E
Lgr5low cells (1 dpi)
PAF WT;Lgr5-EGFP
PAF KO;Lgr5-EGFP
Relative expression (qRT-PCR)
c-Myc CCND1 CD44 Lgr5 Olfm4 Ascl2 CTGF CYR61 Notch Hes1 PTPRG ID1 PTCH
Wnt
ISC
Hippo
Notch
BMP
Hh
F
10Gy, 4 dpi
PAF WT intestine
PAF KO intestine
Relative expression (qRT-PCR)
c-Myc CCND1 Lgr5 Axin2 CD44 Olfm4 Ascl2
G
PAF WT
PAF KO
Normal
2 dpi
4 dpi
7 dpi
c-Myc (N262)
H
PAF WT
PAF KO
1 dpi, 10 Gy
c-Myc (N262)
I
10 Gy, 4 dpi
Myc intensity/ crypt (AU)
WT
KO

Figure S5. Analysis of Regenerating *PAF* KO Intestine and ISCs (related to Figure 4 and Figure 5)

(A, B) No differences in the Lgr5+ cell population of the normal intestines between *PAF* WT and KO mice. Enzymatically dissociated cells Isolated from *PAF* WT;*Lgr5-EGFP* and *PAF* KO;*Lgr5-EGFP* crypts were assessed by FACS (A); Quantification of the ratio of Lgr5+ cells in *PAF* WT and KO mice from at least three independent experiments (B). The representative images were shown from three independent experiments.

(C, D) No differences in Lgr5+ cell populations after IR-injury between *PAF* WT and KO mice. FACS analyzed images from *PAF* WT;*Lgr5-EGFP* and *PAF* KO*; Lgr5-EGFP* crypts (C). Of note, after IR injury, the small number of $Lgr5^{low}$ cells were detected in both *PAF* WT;*Lgr5-EGFP* and *PAF* KO;*Lgr5-EGFP* crypts; Quantification of Lgr5+ cells in the IR-injured crypts (1 dpi, 10 Gy) from at least three independent experiments (D). The representative images were shown from three independent experiments.

(E) Target gene analysis of Wnt, Hippo, Notch, BMP, and Hh signaling pathways in the sorted Lgr5+ cells. FACS-isolated Lgr5+ cells from *PAF* WT;*Lgr5-EGFP* and *PAF* KO;*Lgr5-EGFP* crypts (1 dpi, 10Gy) were analyzed for qRT-PCR. At least three experiments were conducted.

(F) Target gene analysis of Wnt signaling pathways in whole intestine. Whole intestinal crypts (4 dpi, 10Gy) were analyzed for qRT-PCR. At least three experiments were conducted.

(G) Decreased c-Myc expression in normal and regenerating intestinal crypts of *PAF* KO. c-Myc immunostaining (brown, N-262) of the mouse small intestine (*PAF* WT and KO) at the indicated time points. Hematoxylin for nuclear counterstaining (blue). Scale bars=50μm.

(H) Weak expression of Myc in regenerating crypt of *PAF* KO at 1 dpi. Yellow arrowheads indicated that the cells showed high Myc expression in the crypts after IR injury. Scale bars=20μm.

(I) Quantification of Myc intensity in *PAF* WT and *PAF* KO regenerating intestine (10Gy, 4dpi). For quantifying the signal intensity, at least 20 crypts from the indicated genotypes (n=3) were analyzed by image J.

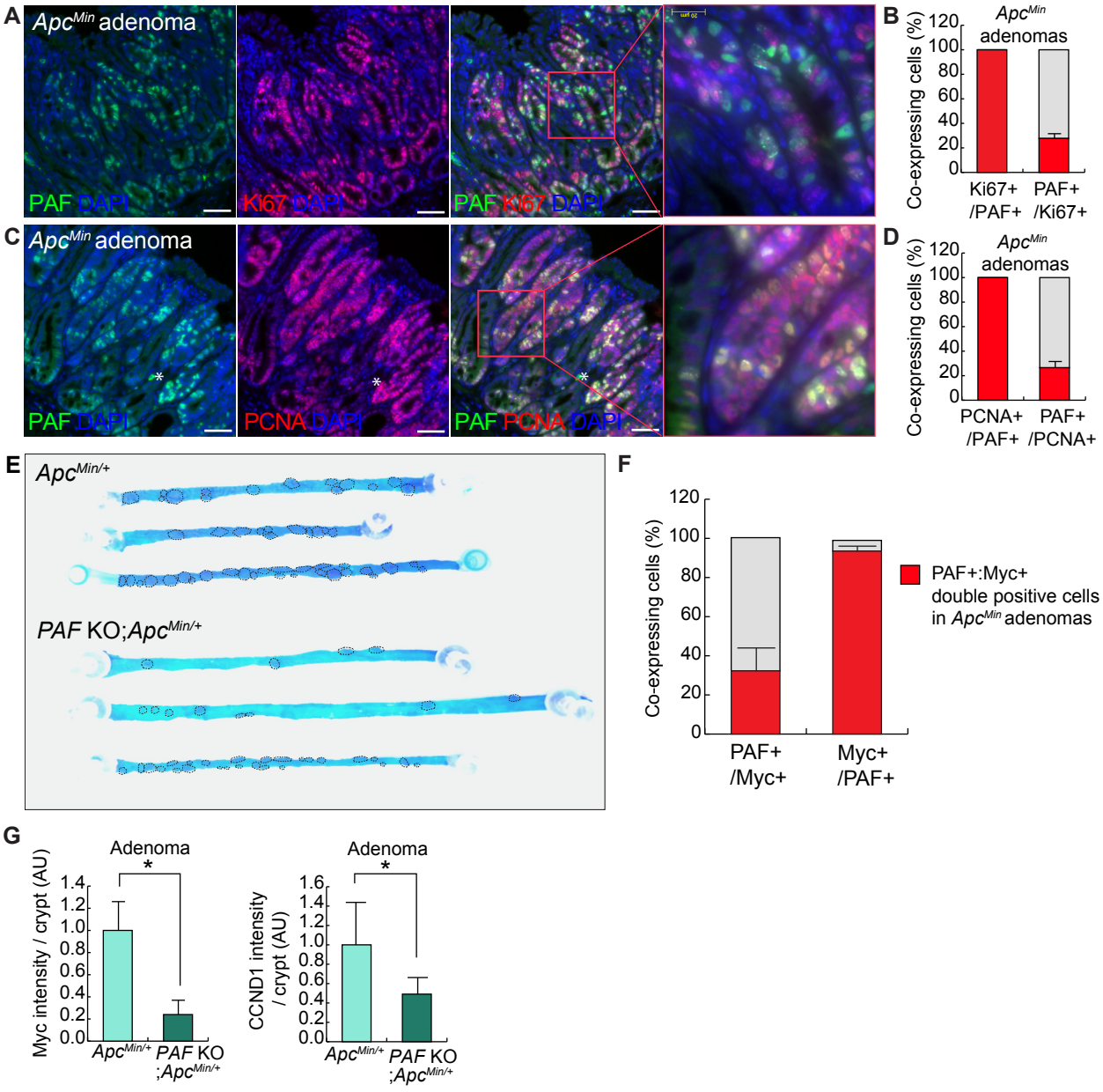
A
Apc^Min adenoma
PAF DAPI
Ki67 DAPI
PAF Ki67 DAPI
B
Apc^Min adenomas
Co-expressing cells (%)
120
100
80
60
40
20
0
Ki67+ /PAF+
PAF+ /Ki67+
C
Apc^Min adenoma
PAF DAPI
PCNA DAPI
PAF PCNA DAPI
D
Apc^Min adenomas
Co-expressing cells (%)
PCNA+ /PAF+
PAF+ /PCNA+
E
Apc^Min/+
PAF KO;Apc^Min/+
F
Co-expressing cells (%)
PAF+ /Myc+
Myc+ /PAF+
PAF+:Myc+ double positive cells in Apc^Min adenomas
G
Adenoma
Myc intensity / crypt (AU)
1.4
1.2
1.0
0.8
0.6
0.4
0.2
0.0
Apc^Min/+
PAF KO ;Apc^Min/+
Adenoma
CCND1 intensity / crypt (AU)
1.6
1.4
1.2
1.0
0.8
0.6
0.4
0.2
0.0
Apc^Min/+
PAF KO ;Apc^Min/+

Figure S6. Reduced Intestinal Tumorigenesis by *PAF* KO (related to Figure 6)

(A, B) PAF and Ki67 co-expression analysis in Apc^{Min} adenomas. The representative images of PAF and Ki67 co-immunostaining of Apc^{Min} (16 weeks) adenomas (A); Quantification of co-expressing cells (B). 100% of PAF+ cells were colocalized with Ki67 staining (N≥500). 27.68% of Ki67 expressing cells (Ki67+) were colocalized with PAF expression (N≥500). Scale bars=50μm.

(C, D) PAF and PCNA co-expression analysis of Apc^{Min} adenomas. Representative images of PAF and Ki67 co-immunostaining of Apc^{Min} (16 weeks) adenomas (C); Quantification of co-expressing cells (D). 100% of PAF+ cells were co-localized with PCNA staining (N≥500). 26.49% of PCNA expressing cells (PCNA+) were co-localized with PAF expression (N≥500). Asterisk mark non-specific staining signals. Scale bars=50μm

(E) Decreased the development of *Apc* mutation-driven adenomas in *PAF* KO mice. The representative image of the whole small intestine from $Apc^{Min/+}$ and *PAF* KO;$Apc^{Min/+}$ mice.

(F) PAF and Myc co-expression analysis in Apc^{Min} adenomas. 33.96% of Myc-expressing cells (Myc+) were co-localized with PAF+ cells (N≥400). 97.25% of PAF+ cells were co-localized with Myc+ cells (N≥150).

(G) Quantification of *Myc* and *CCND1* intensity in *PAF* WT*;* Apc^{Min} and *PAF* KO; *;* Apc^{Min} adenomas (16 weeks old). For quantifying the signal intensity, at least 15 adenomas from the indicated genotypes (n=3) were analyzed by image J.

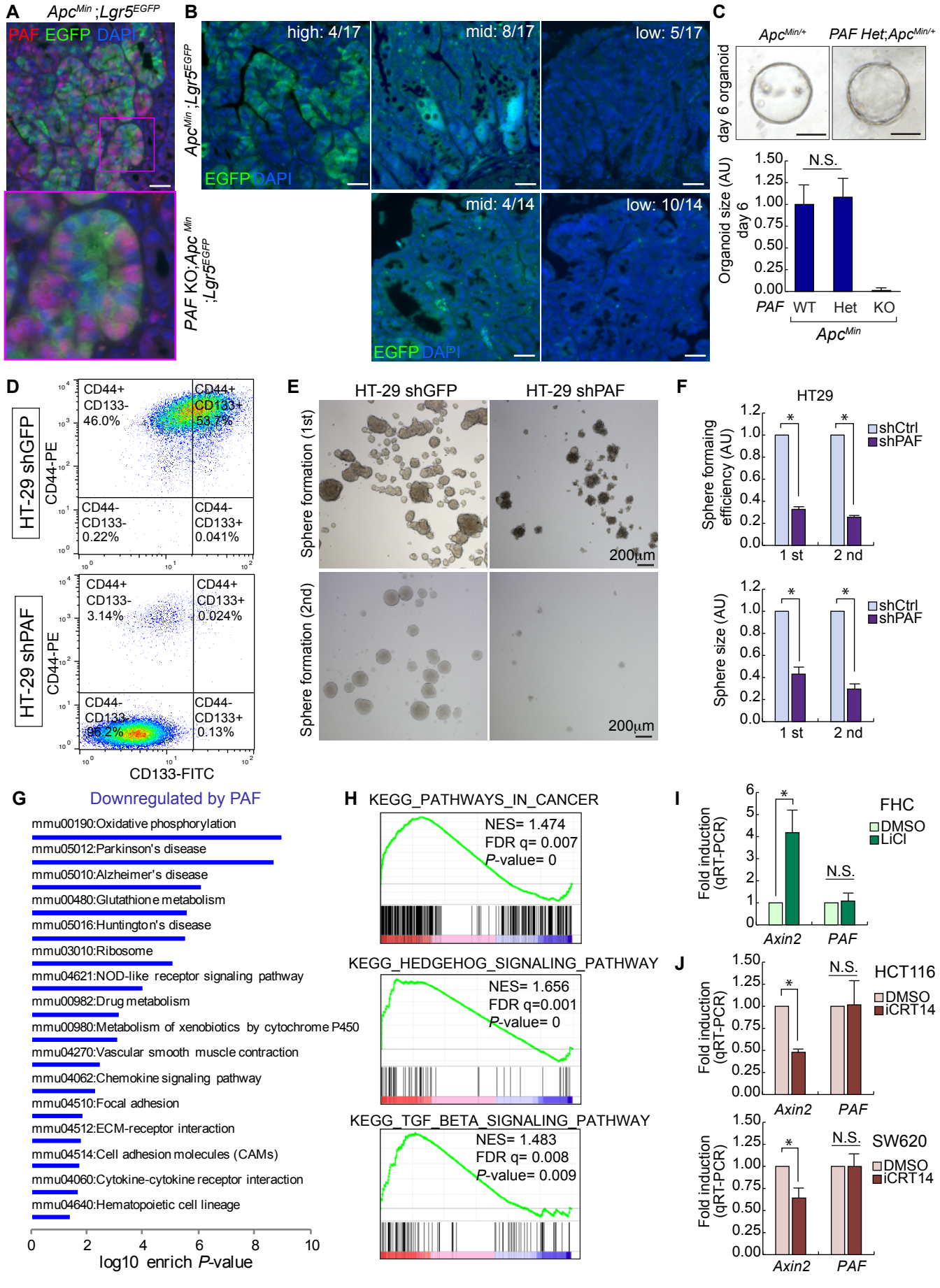
A
Apc^Min ;Lgr5^EGFP
PAF EGFP DAPI
PAF KO;Apc^Min ;Lgr5^EGFP
B
Apc^Min ;Lgr5^EGFP
high: 4/17
mid: 8/17
low: 5/17
EGFP DAPI
mid: 4/14
low: 10/14
C
Apc^Min/+
PAF Het;Apc^Min/+
day 6 organoid
Organoid size (AU) day 6
N.S.
PAF WT Het KO
Apc^Min
D
HT-29 shGFP
CD44-PE
CD44+ CD133- 46.0%
CD44+ CD133+ 53.7%
CD44- CD133- 0.22%
CD44- CD133+ 0.041%
HT-29 shPAF
CD44+ CD133- 3.14%
CD44+ CD133+ 0.024%
CD44- CD133- 96.2%
CD44- CD133+ 0.13%
CD133-FITC
E
HT-29 shGFP
HT-29 shPAF
Sphere formation (1st)
Sphere formation (2nd)
200μm
F
HT29
Sphere formaing efficiency (AU)
shCtrl
shPAF
1 st
2 nd
Sphere size (AU)
G
Downregulated by PAF
mmu00190:Oxidative phosphorylation
mmu05012:Parkinson's disease
mmu05010:Alzheimer's disease
mmu00480:Glutathione metabolism
mmu05016:Huntington's disease
mmu03010:Ribosome
mmu04621:NOD-like receptor signaling pathway
mmu00982:Drug metabolism
mmu00980:Metabolism of xenobiotics by cytochrome P450
mmu04270:Vascular smooth muscle contraction
mmu04062:Chemokine signaling pathway
mmu04510:Focal adhesion
mmu04512:ECM-receptor interaction
mmu04514:Cell adhesion molecules (CAMs)
mmu04060:Cytokine-cytokine receptor interaction
mmu04640:Hematopoietic cell lineage
log10 enrich P-value
H
KEGG_PATHWAYS_IN_CANCER
NES= 1.474
FDR q= 0.007
P-value= 0
KEGG_HEDGEHOG_SIGNALING_PATHWAY
NES= 1.656
FDR q=0.001
P-value= 0
KEGG_TGF_BETA_SIGNALING_PATHWAY
NES= 1.483
FDR q= 0.008
P-value= 0.009
I
FHC
DMSO
LiCl
Fold induction (qRT-PCR)
Axin2
PAF
J
HCT116
DMSO
iCRT14
SW620

Figure S7. Reduced CRC Cell Stemness by *PAF* KO (related to Figure 7)

(A) PAF and Lgr5 (GFP) immunostaining in *Apc*^{Min} adenomas. Scale bars=100μm.

(B) Analysis of Lgr5 expression in adenomas from *Apc*$^{Min/+}$*;Lgr5-GFP* and *PAF* KO;*Apc*$^{Min/+}$*;Lgr5-EGFP* (16 wk old). Scale bars=100μm.

(C) No differences in the cystic organoid growth between *Apc*$^{Min/+}$ and *PAF* Het;*Apc*$^{Min/+}$ (N≥30 cystic organoids were analyzed). Scale bars=100μm.

(D) PAF depletion reduced expression of CD44 and CD133 in CRC cell line. FACS analysis for CD44 and CD133 using shGFP (control) and shPAF of HT-29 cells.

(E, F) PAF depletion reduced sphere formation in CRC cell line. Representative images of sphere formation assay (1st and 2nd) using shGFP (control) and shPAF of HT-29 cells (E); Quantification of the number and the size of spheres (F). Scale bar=200μm.

(G) Significantly PAF downregulated signaling pathways identified by GSEA analysis (KEGG) using RNA-seq result. $P<0.05$.

(H) Gene set enrichment analysis (GSEA) for PAF activated signaling pathways using KEGG method. NES, normalized enrichment score; FDR, False detection rate; P-value, Nominal P-value.

(I) No differences in PAF expression upon Wnt activation. FHC (normal intestinal epithelial cell line) cells were treated with LiCl, an inhibitor of GSK3 for β-catenin stabilization (Wnt agonist)(25 mM, 24h) and analyzed for qRT-PCR. Expression of Axin2 was used as a positive control.

(J) No differences in PAF expression upon Wnt inactivation. HCT116 and SW620 (CRC cell lines) cells were treated with iCRT14 (Wnt signaling inhibitor) (100 μM, 24h) and analyzed for qRT-PCR.

Table S3. Primer sequence information (Related to STAR Methods)

List of all primer sequences used for qRT-PCR and ChIP assays

qRT-PCR primer		
Murine gene	**Forward primer (5' to 3')**	**Reverse primer (5' to 3')**
PAF	TGTGATCAGGTTGCAAAGGA	TTCAGGCTGTCCCCTAAAGA
c-Myc	ATGCCCCTCAACGTGAACTTC	GTCGCAGATGAAATAGGGCTG
CCND1	GCGTACCCTGACACCAATCTC	CTCCTCTTCGCACTTCTGCTC
Axin2	TGACTCTCCTTCCAGATCCCA	TGCCCACACTAGGCTGACA
CD44	CACCATTGCCTCAACTGTGC	TTGTGGGCTCCTGAGTCTGA
CD133	TCGTACTGGTGGCTGGGTGGC	ACCACAAGGATCATCAATATC
Lgr5	ACCCGCCAGTCTCCTACATC	GCATCTAGGCGCAGGGATTG
Olfm4	TGGCCCTTGGAAGCTGTAGT	ACCTCCTTGGCCATAGCGAA
Ascl2	AAGCACACCTTGACTGGTACG	AAGTGGACGTTTGCACCTTCA
CTGF	AGCCTCAAACTCCAAACACC	CAACAGGGATTTGACCAC
CYR61	GATGACCTCCTCGGACTCGAT	CGTGCAGAGGGTTGAAAAGAA
Notch	TCAGTGTGACCCAGACCTTG	CAAAAGGCCAGAAAGAGCTG
Hes1	GGTATTTCCCCAACACGCT	GGCAGACATTCTGGAAATGA
PTPRG	CGGAGGTTACTGGAACCGTG	CAGGGTCCCCACATAGCCT
ID1	CTGAACGGCGAGATCAGTG	TTTTCCTCTTGCCTCCTGAA
PTCH	GCAAGTTTTTGGTTGTGGGT	TTCTCGACTCACTCGTCCAC
HPRT1	TCAGTCAACGGGGGACATAAA	GGGGCTGTACTGCTTAACCAG
18S	AAGTCCCTGCCCTTTGTACACA	GATCCGAGGGCCTCACTAAAC
Human gene	**Forward primer (5' to 3')**	**Reverse primer (5' to 3')**
PAF	CCAGGGTAAACAAGGAGACG	CAGGAAGCAGTGGCTTAGGA
Axin2	AGCTTACATGAGTAATGGGG	AATTCCATCTACACTGCTGTC
HPRT1	ACCCTTTCCAAATCCTCAGC	GTTATGGCGACCCGCAG
Primers for ChIP assays		
Murine gene	**Forward primer (5' to 3')**	**Reverse primer (5' to 3')**
c-Myc-TBE	ATCTGATCAGGGCCGATTT	GAGCCTGCAGAGACCCTAGAA
CCND1-TBE	CTTTTCTCTGCCCGGCTTT	TCTGGAGGCTGCAGGACTT
GAPDH	CCTTAGCCCTGAGCTGTGTC	ATGTTTTCTGGGGTGCAAAG